LASER INTERFEROMETER GRAVITATIONAL WAVE OBSERVATORY
- LIGO -
CALIFORNIA INSTITUTE OF TECHNOLOGY
MASSACHUSETTS INSTITUTE OF TECHNOLOGY

Technical Note	**LIGO-T11XXXXX–vX**	2012/09/24

Detector Characterization Tools for Interferometer Commissioners

Elizabeth Davison
Mentors: Jameson Rollins and Rana Adhikari

California Institute of Technology
LIGO Project, MS 18-34
Pasadena, CA 91125
Phone (626) 395-2129
Fax (626) 304-9834
E-mail: info@ligo.caltech.edu

Massachusetts Institute of Technology
LIGO Project, Room NW22-295
Cambridge, MA 02139
Phone (617) 253-4824
Fax (617) 253-7014
E-mail: info@ligo.mit.edu

LIGO Hanford Observatory
Route 10, Mile Marker 2
Richland, WA 99352
Phone (509) 372-8106
Fax (509) 372-8137
E-mail: info@ligo.caltech.edu

LIGO Livingston Observatory
19100 LIGO Lane
Livingston, LA 70754
Phone (225) 686-3100
Fax (225) 686-7189
E-mail: info@ligo.caltech.edu

http://www.ligo.caltech.edu/

Abstract

The Laser Interferometer Gravitational-Wave Observatory (LIGO) detectors are dual-recycling interferometers with Fabry-Pérot arm cavities four kilometers in length. Complex control and data acquisition systems for these instruments are prototyped at the 40 meter interferometer on the Caltech campus. With the development of increasingly intricate subsystems, it has become important for the commissioners working at the 40 meter lab to have an accessible, effective overview of the instrument's behavior. This project required consultation with each scientist and an overall understanding of the interferometer in order to refine the considerable amount of information from the data channels into useful plots. Code that had been used for a full-scale interferometer website was modified to suit the 40 meter lab's objectives. The result of this project is a regularly updated website that contains calibrated plots of relevant channels and images of monitoring screens. It can be further adapted by the scientists at the 40 meter lab as the need arises and will be a helpful and informative tool.

Contents

1 Introduction

1.1 Gravitational Waves

The Laser Interferometer Gravitational-Wave Observatory (LIGO) is an effort to produce a worldwide network of instruments capable of detecting gravitational waves. Einstein's theory of relativity posits that gravitational waves are caused by coherent motion of massive objects. Gravitational waves that arise from events generated on Earth are not large enough to be detected, so scientists must rely on naturally occurring astronomical events to produce measurable waves. The 1993 Nobel Prize was awarded to Hulse and Taylor for indirectly validating the existence of gravitational radiation by observing the inspiral rate of binary pulsar PSR1913+16. [1] When the advanced LIGO project constructs a detector that is precise enough to detect gravitational waves, a new era in experimental astrophysics will begin. Gravitational waves pass through matter without excessive scattering, so gravitational wave detectors will provide a novel perspective on the universe.

When a gravitational wave propagates through space, it can be described as a combination of cross and plus polarizations. The wave acts on the plane of space-time perpendicular to the direction of propagation, elongating space along one axis and compressing it along the other. [2] The orientation of the quadrupolar axes is determined by the polarization. For the Earth-Sun system and an observer in the x-y plane, the amplitude of the resultant gravitational radiation (in the plus polarization) can be obtained:

$$|h| = -\frac{4G^2 m_1 m_2}{Rc^4 r}$$

Here, R is the distance from the center of mass of the system to the observer, $m_1 m_2$ is the product of the masses in the Earth-Sun system, r is the radius of the orbit (under the assumption that the orbit is circular), and $|h|$ is the gravitational wave amplitude in terms of strain ($\frac{\Delta L}{L}$). For this system, the value of $|h|$ is 10^{-26}.[3] In the case of a neutron star binary in one of the closest galaxies, the calculated value of $|h|$ is only about 10^{-21}.[4] However, if the gravitational wave acts over a kilometer, the strain will be approximately 10^{-18}.

1.2 The LIGO Experiment

In the initial LIGO experiment (iLIGO), three interferometers were constructed in Washington and Louisiana. The smaller 40 meter lab, situated on the Caltech campus, is used for development, testing and implementation of control and data systems for the advanced LIGO (aLIGO) project. aLIGO aims to increase the sensitivity of iLIGO by a factor of ten, primarily by improving seismic isolation and control systems and reducing the effect of quantum shot noise. A long term goal of the project, and a necessary step towards using the interferometers for observation instead of detection, is to have a functioning network of instruments all over the globe. This system would make it possible to isolate noise from local sources and accurately triangulate the positions of gravitational wave sources.

The aLIGO detectors are dual-recycling Michelson interferometers with four kilometer Fabry-Pérot cavities as arms. Mirrored test masses are hung from several stages of seismic isolation at the end of each arm. A passing gravitational wave will change the cavity length by a

thousandth of the radius of a neutron. At this level of precision, it is necessary that the subsystems do not introduce excess noise into the measurements.

2 The 40 Meter Lab

The aLIGO interferometers contain a multitude of subsystems that ensure the optics are stabilized, the cavity lengths are resonant, and unnecessary and potentially obfuscating noise is minimized. The control and data systems for the aLIGO interferometers are prototyped at the 40 meter site. Models for the entire system are compiled onto several processors that run the code and subsequently interact with the interferometer through ADCs and DACs. A diagram of the overall layout of the 40 meter interferometer can be seen in Figure 1. [5] The complexity of the systems at the 40 meter lab is constantly increasing as new control

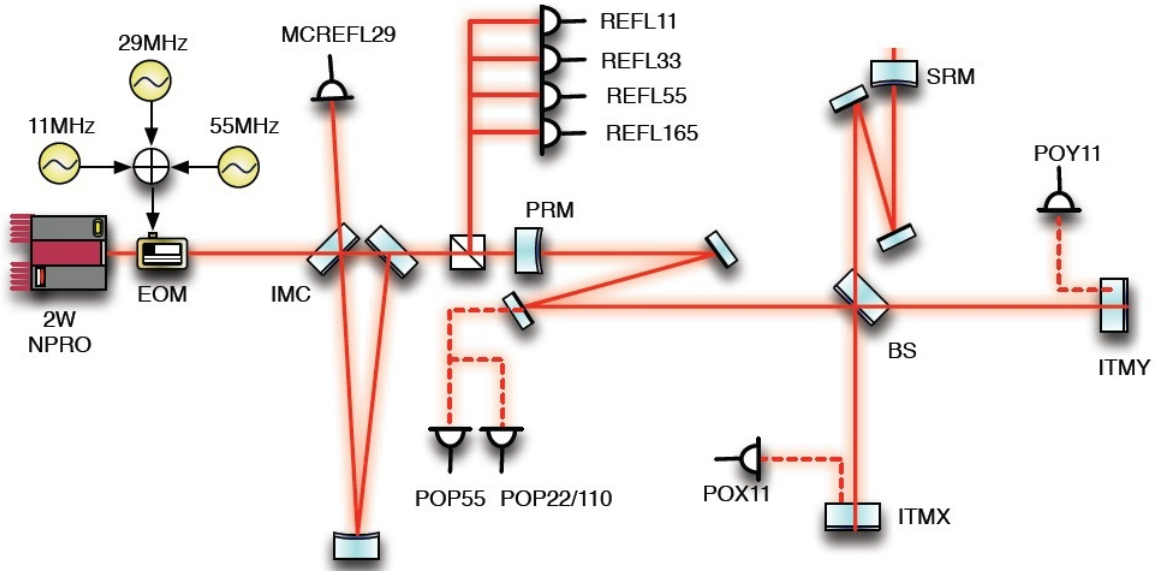

Figure 1: The layout of the 40 meter interferometer.

technologies are implemented. As a result, there is a growing need for an easily accessible summary of the status of the interferometer and associated components. Thousands of data channels continuously monitor the interferometer and its environment with sampling rates up to 16 kHz. Some of these are calibrated, but most are in units of counts and are incomprehensible except to the practiced eye. The purpose of this project is to provide an accessible website that depicts clear, informative plots that can be checked to determine the current state of the interferometer and its subsystems.

3 Pound Drever Hall Locking

The Pound-Drever-Hall technique is implemented at the 40 meter lab to lock the interferometer cavities to their respective resonant lengths. Carrier light of frequency $\nu = \frac{\omega}{2\pi}$ has

an electric field:

$$E = E_0 e^{i\omega t}$$

At the 40 meter, a triple-resonant electro-optic modulator (EOM) modulates the phase of the carrier light, introducing frequency sidebands with frequency $\frac{\omega \pm \Omega}{2\pi}$, where Ω = 11, 29.5 and 55 MHz. The modulation is of the form $\beta \sin(\omega t)$ and the resulting electric field equation is:

$$E_i = E_0 e^{i(\omega t + \beta \sin(\Omega t))} \approx E_0 e^{i\omega t}\left[1 + \frac{\beta}{2} e^{i\Omega t} - \frac{\beta}{2} e^{-i\Omega t}\right]$$

When the modulated light enters an optical cavity, some is reflected to a photodiode sensor. The reflection coefficient for a cavity with no losses is:

$$F = \frac{r(e^{i\phi} - 1)}{1 r^2 e^{i\phi}}$$

Where r is the reflection coefficients of each mirror and ϕ is the phase by which the light increases by during its time in the cavity, $\frac{2\omega L}{c}$. This can be multiplied by E_i to obtain E_r and the reflected power, which is proportional to the photodiode voltage. A mixer compares the modulation signal with the signal from the photodetector and isolates constituents at the modulation frequency. The sign of the error signal from the mixer will change on either side of resonance and provides the signal for the actuators on the cavity mirror. Fluctuations in the cavity length can thus be detected as fluctuations in the reflected light and input into a feedback loop to control cavity length. [6]

4 Interferometer Subsystems

4.1 Pre-Stabilized Laser

The pre-stabilized laser (PSL) is a 2 Watt nonplanar ring oscillator (NPRO) with λ = 1064 nm. The PSL subsystems refine the carrier beam into a stable TEM_{00} mode. The frequency stabilization servo (FSS) consists of a feedback loop that utilizes the PDH technique to compare the frequency of the NPRO with a reference cavity. The pre mode cleaner (PMC) then passively filters light to reduce fluctuations. A triple-resonant EOM then modulates the carrier beam with radio frequency sidebands at 11, 29.5 and 55 MHz in order to facilitate Pound-Drever-Hall locking in the interferometer cavities. Figure 2 is an overview of the PSL table that details the beam path and main components.[7] The pre mode cleaner is a triangular ring cavity that reduces the higher order mode content of the carrier beam and passively filters above the cavity pole, about 450 kHz. The current version of the PMC plot is shown in Figure 3. The reflected power from the PMC is used by the control system to determine whether the PMC is a resonant length. In this instance of PDH locking, the cavity is locked to the wavelength of the carrier beam. Light from the NPRO will only resonate in the cavity if the cavity length is an integer number of half-wavelengths. The RF sidebands are reflected and this power is measured by a radio frequency photodiode (RFPD). The error signal from the RFPD is used as the signal in a feedback loop to actuate on a

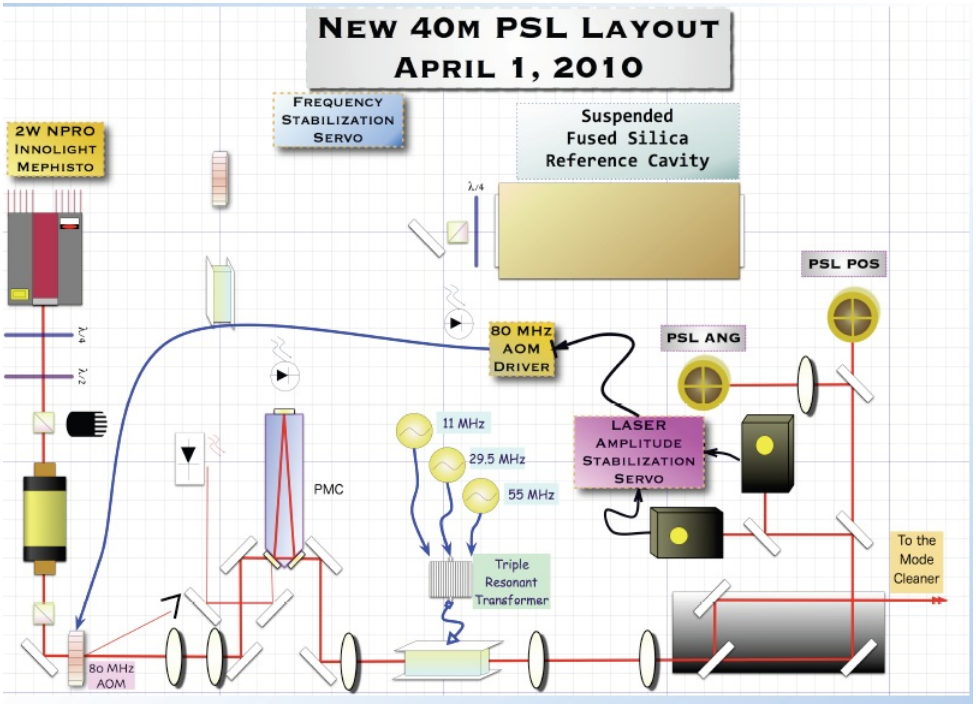

Figure 2: The layout of the PSL table at the 40 meter interferometer. The sources for the frequency and intensity servos are picked off before the PMC, which acts as a low pass filter before the beam inters the input optics.

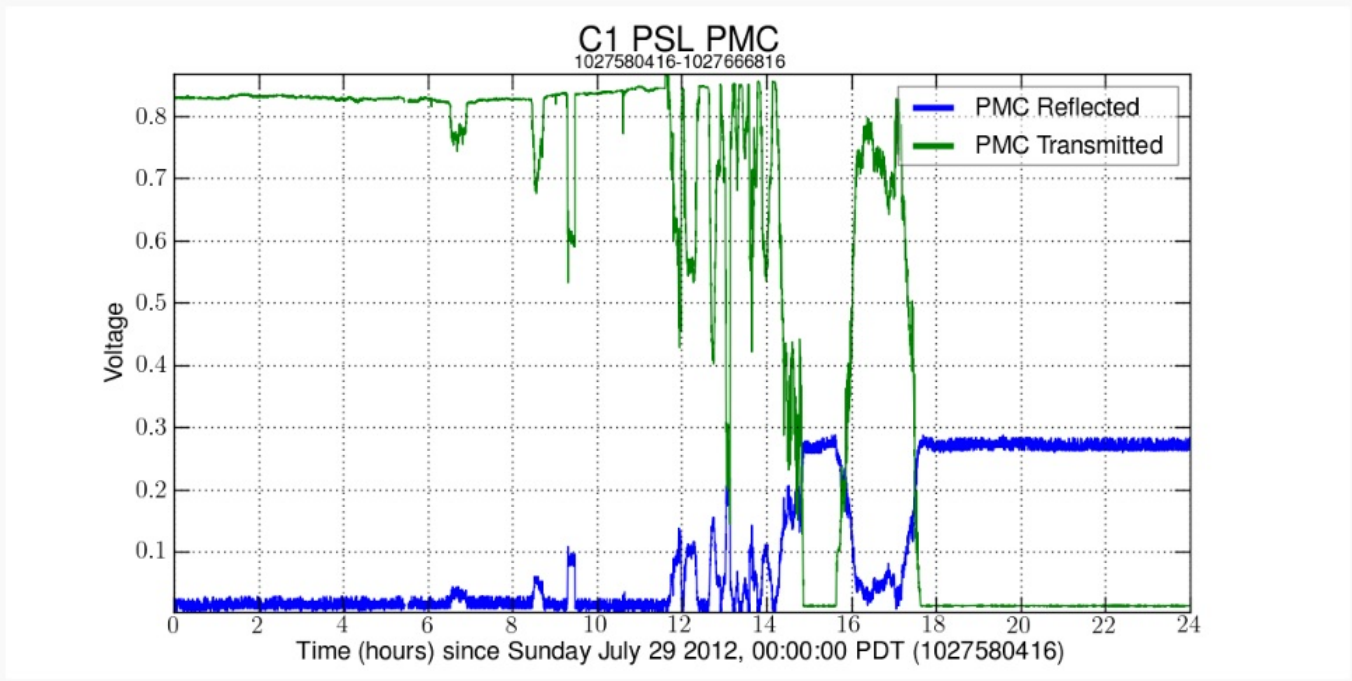

Figure 3: The PMC reflected and transmitted power. They are both output in terms of voltage but may need to be modified so they are in Watts.

mirror and bring the PMC back into resonance. Although this plot would be more intuitive if the channels were calibrated in Watts, it is informative without this calibration. The PZT drives the curved mirror at one vertex of the PMC (in Figure 2, this is the upper mirror in the PMC) in order to maintain resonance in the cavity. The error signal from the reflected PMC power is used by the control system in order to determine the amount of actuation the PZT should exert on the mirror. The FSS uses PDH locking with the Mode Cleaner length error to stabilize the PSL wavelength. Figure 4 depicts the output voltage of the PZT alongside the fast and slow FSS channels. The final plot on the PSL page is a temperature

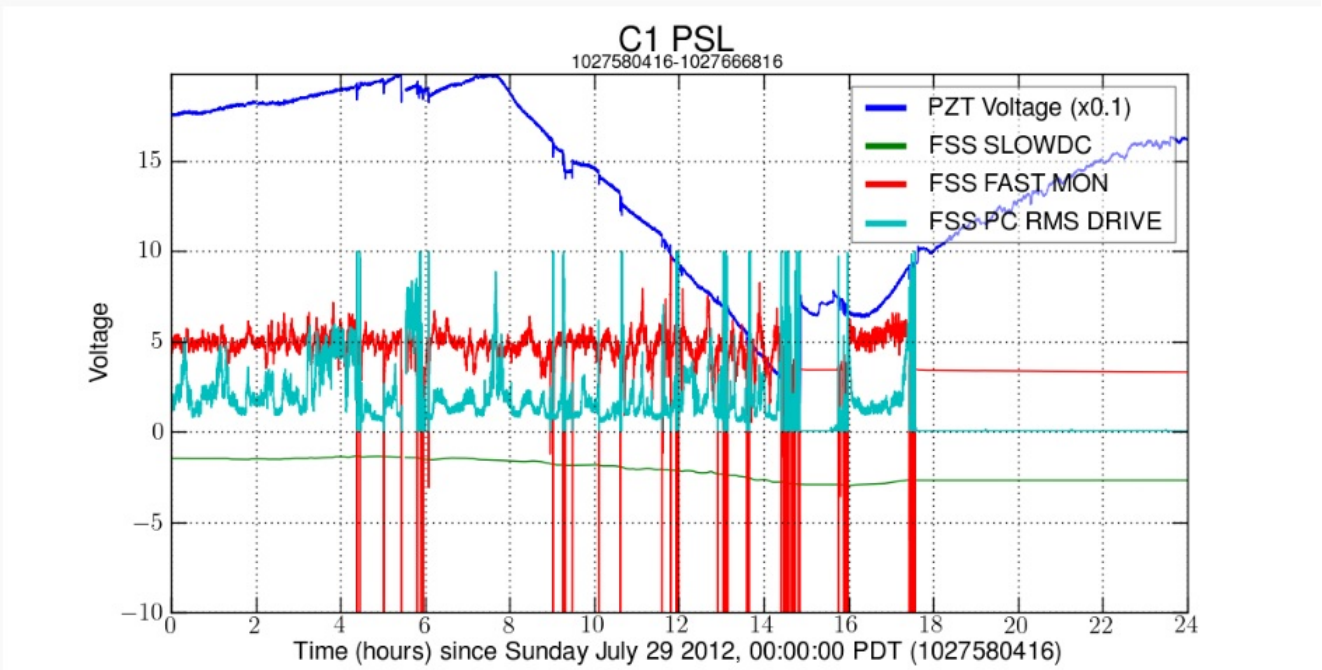

Figure 4: The fast and slow FSS channels, and the trace of the voltage in the PZT. All channels are calibrated in Volts and the PZT voltage has a multiplier of 0.1 so that it will remain within comparable limits (0-25 V).

plot that can be referenced to see what is occurring in the PSL environment. It includes time-series plots of the temperature on the table and the reference cavity temperature (RC Temperature), as seen in Figure 5.These are essential environmental monitoring systems that can be consulted to determine the status of the PSL.

4.2 Input Mode Cleaner

The input mode cleaner (IMC) is a suspended triangular Fabry-Pérot cavity that further refines the light from the PSL table and stabilizes it in TEM_{00} mode. It has an optical half-length of 13.5 meters and contains three LIGO small optic suspensions (SOS). There is one curved and two plane optics. The mode cleaner is essential because it filters out higher order modes and frequency fluctuations that would reduce the efficacy of the experiment. The plane mirrors also act as polarization selectors, because they have a transmission coefficient ten times higher for horizontal polarization. The RF sidebands are also resonant in the

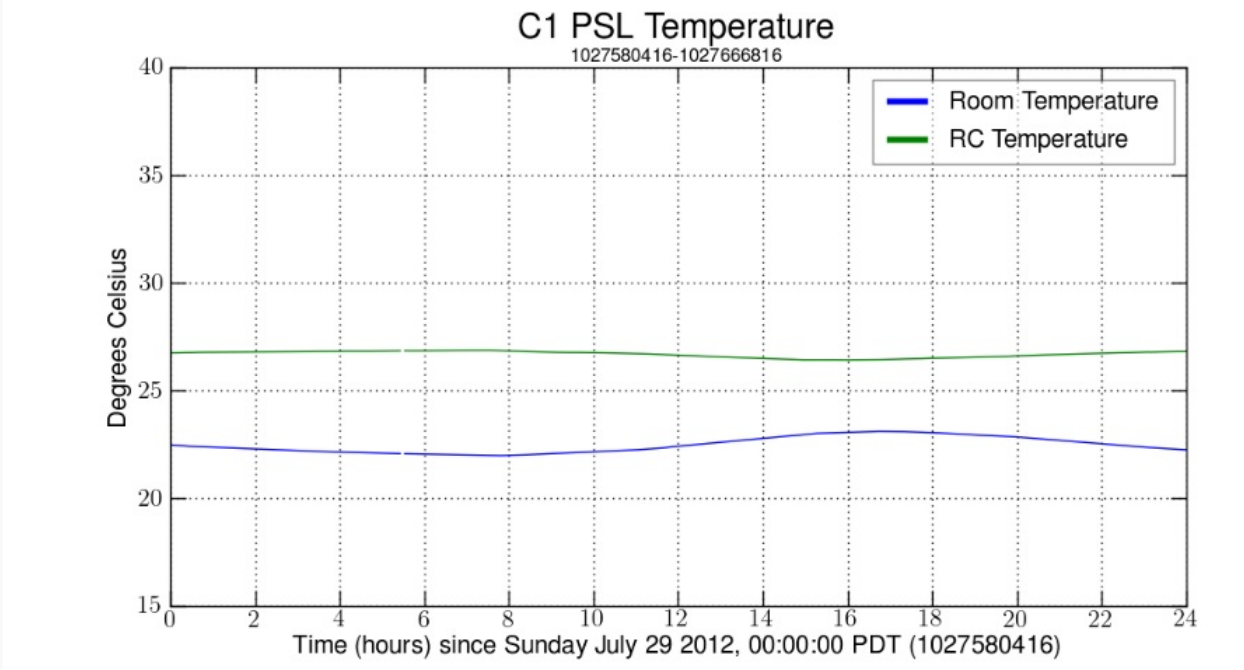

Figure 5: The temperature on the PSL table and in the thermally insulated reference cavity. The reference cavity is at a slightly higher temperature because it is temperature-controlled.

IMC and are thus transmitted to the interferometer. As in the pre mode cleaner, the mode cleaner's reflected and transmitted beams are monitored and the reflected power is the source of a feedback loop that controls the cavity length.[8] The signal from the reflected RFPD is demodulated and used to fabricate an error signal that can be used to stabilize the IMC cavity length. Figure 6 is the reflected and transmitted power of the mode cleaner in terms of Volts. Additionally, there are plots of the pitch and yaw of the IMC components, as shown in Figure 7. Two wave front sensors output data about the beam that can be converted to the pitch and yaw of the plane mirrors and one quadrant photodiode sensor outputs the pitch and yaw of the curved mirror. These channels can provide information about whether the mode cleaner is aligned properly and consequentially whether it is refining the input mode correctly.

4.3 Length Sensing and Control

The length sensing and control (LSC) schemes at the 40 meter lab are tested and improved for their final implementation at the aLIGO interferometers. The purpose of the LSC system is to lock the optical cavity lengths to the carrier wavelength. Length sensing utilizes the RF sidebands, which are resonant in different optical cavities. Figure 8 depicts the resonance profile of each frequency of light used at the 40 meter. The 33 MHz sidebands resonate in the power recycling cavity (PRC), while the 166 MHz sidebands resonate in the PRC and signal recycling cavity (SRC) and represent the entire Michelson length (MICH). The DC monitors are located at the symmetric port (REFL), asymmetric port (AS), the transmitted ports for the X and Y arms (TRX and TRY), and various pick-off ports. The signals from these

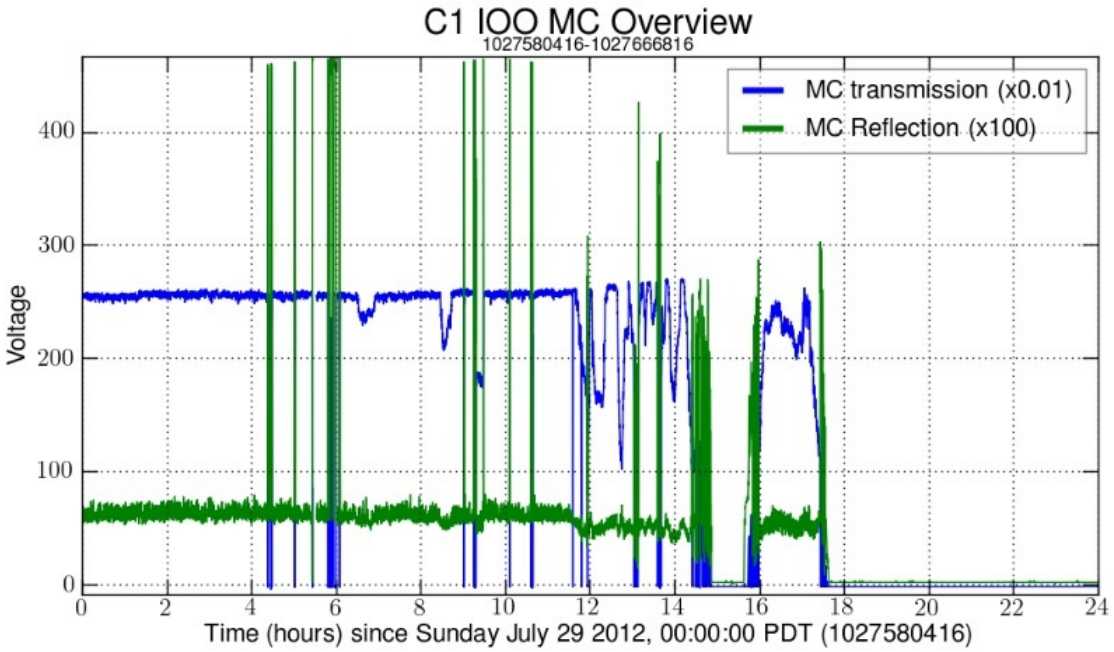

Figure 6: Mode cleaner reflected and transmitted power. They are both output in terms of voltage but may need to be modified so they are in Watts.

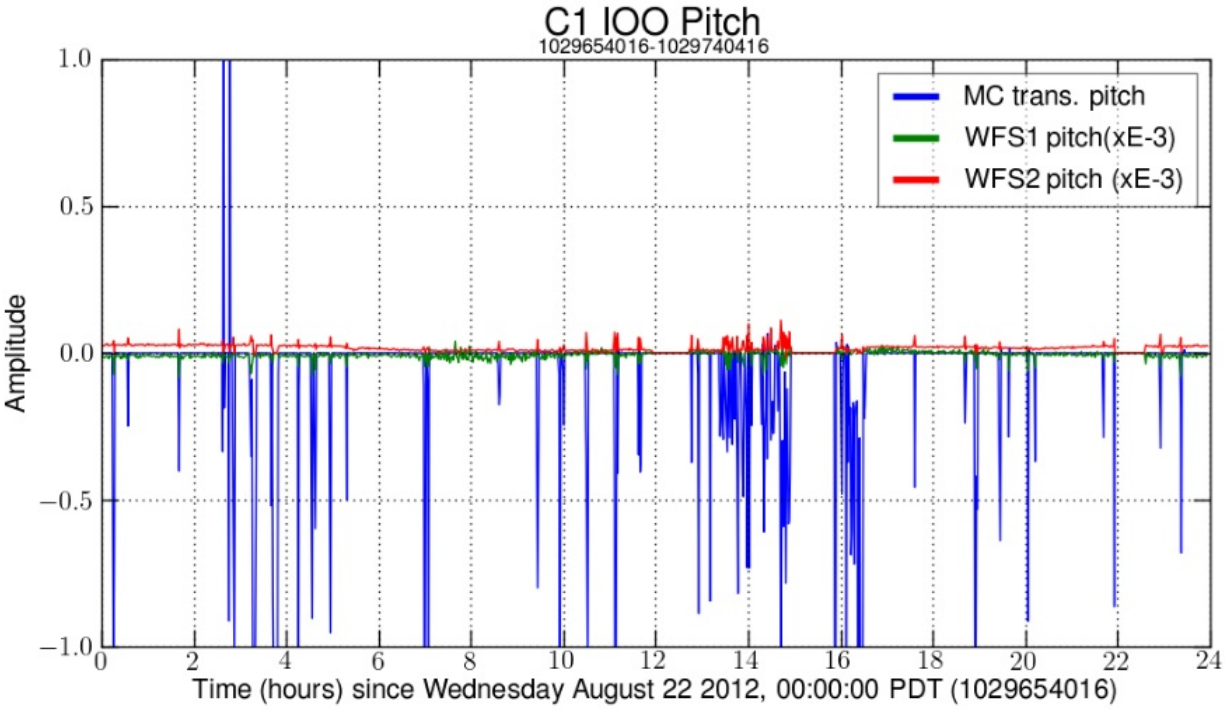

Figure 7: This depicts the pitch of the three mode cleaner mirrors. WFS1 and WFS2 are the mirrors that are fixed, and MS trans is the curved mirror at the vertex.

ports are demodulated and input into a sensing matrix. The traces in Figure 9 represent the power at five of these detectors over time. The length control system at the 40 meter uses a control basis comprised of the following length degrees of freedom: differential arm (DARM), common arm (CARM), power recycling cavity length (PRCL), signal recycling cavity length (SRCL), MICH, and MC length. All the length DOFs are initially arbitrary. In lock acquisition, each DOF is brought to its optimal operating point. An output matrix converts the control basis to the optical basis (ETMX, ITMX, etc.), which adjusts the positions of the optics. Figure 10 depicts the time series of the DARM, CARM, PRCL, SRCL, and MICH feedback values. If these are close to zero, the interferometer is closer to being in lock.

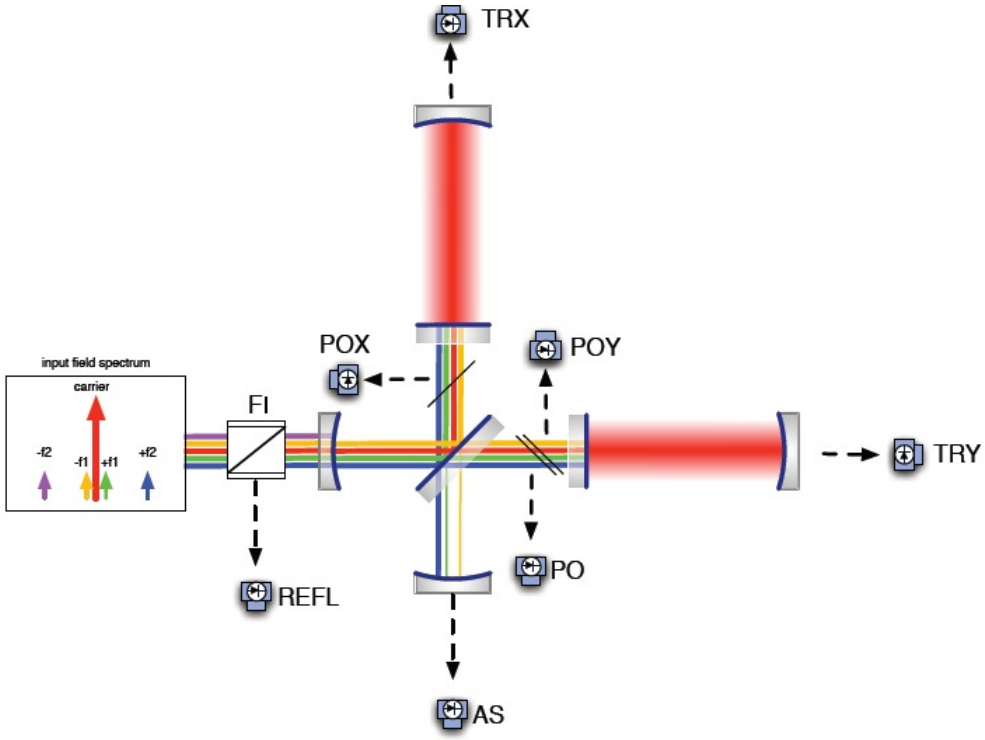

Figure 8: DC resonance profile of the 40 meter interferometer. POX, TRX, AS, etc. are the locations of the DC monitors.

4.4 Suspensions

All of the main mirrored components in the interferometer are suspended in single pendula and have a complex array of monitoring systems. There are three mirrors in the mode cleaner, end and input test masses for the X and Y arms, a power recycling mirror, a beam splitter, and a signal recycling mirror. Optical sensor and electromagnetic motor (OSEM) channels exist for each of the optics and provide detailed information on their positions. The OSEMs consist of magnetic actuators that gently adjust the position of the mirrors and LED and photodiode shadow sensors. There are five of these for each mirror (upper left/right, lower left/right, and side) and each channel is calibrated in units of micrometers. The coil-

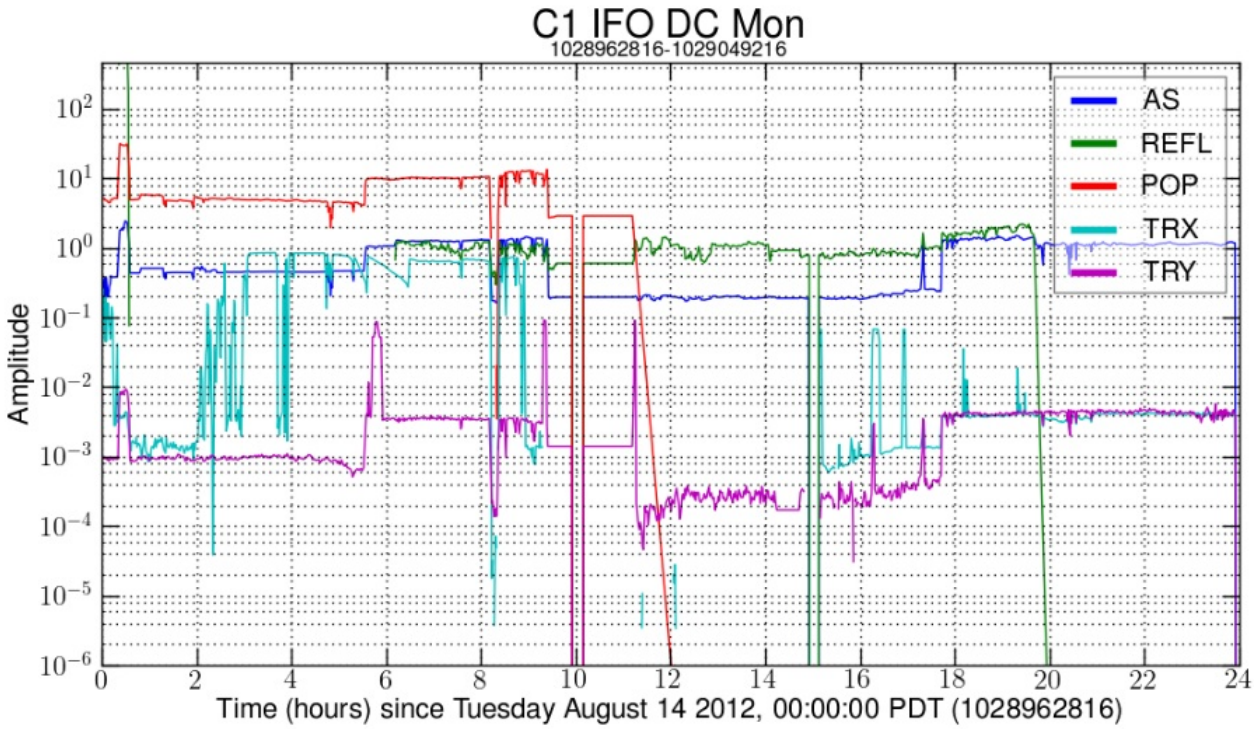

Figure 9: Traces of the power in the five primary DC monitors. Along with the POX and POY detectors, these comprise the length sensing system.

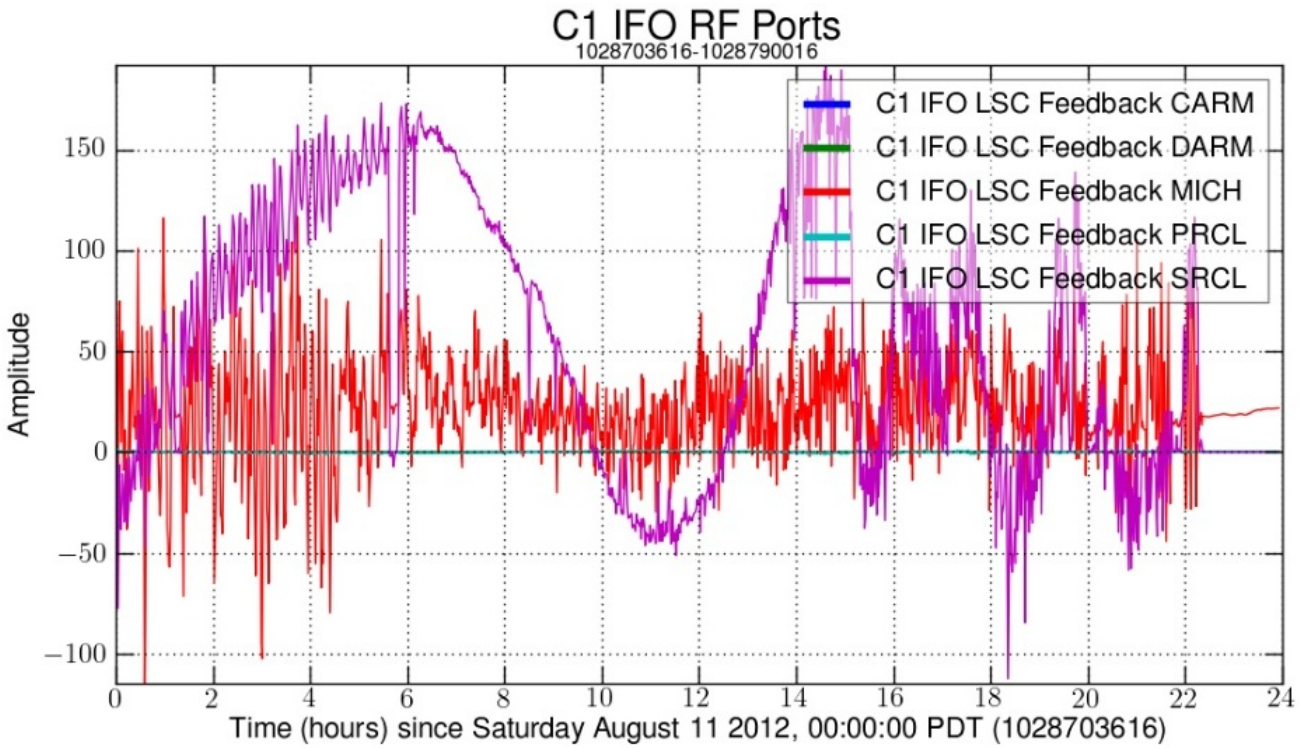

Figure 10: Time series of the feedback values for the length degrees of freedom.

current actuators can control pitch, yaw, side, and longitudinal degrees of freedom for each optic. Time series plots of these channels are extremely informative because OSEM channels are precise at determining when the interferometer is misaligned, as seen in Figure 11. If a large displacement is seen in all of the OSEM channels for each optic, it is clear that an earthquake or other large event took place. This is quite helpful because such occurrences cause the interferometer to come out of lock. If the OSEMs in only one chamber were affected, a more localized event must have occurred. In Figure 12, 40 meter scientists were experimenting with ETMX in the afternoon, so the traces depict fluctuations from about 1:00 to 5:00 PM. Another essential component of the suspension subsystem, optical levers (oplevs) give information about the angular position of the mirrors and can control pitch and yaw. [9] There are oplevs for each mirror in the core optics system, but the Mode Cleaner mirrors do not have oplevs. Oplevs are auxiliary lasers that reflect off of the core optics at an angle, are sensed by a photodetector, and provide feedback for the mirrors angular control. A plot of the yaw of all the core optics is shown in Figure 13. These channels are not calibrated yet but will eventually be in terms of radians.

4.5 Physical and Environmental Monitoring Systems

The Physical and Environmental Monitoring Systems (PEM) consist of signals from the seismic and microphone channels, weather reports, and particle counts. It is important for the PEM to be accessible because it is the first system to consult when something unusual happens that is not related to misalignment. If there was a thunderstorm or excessive

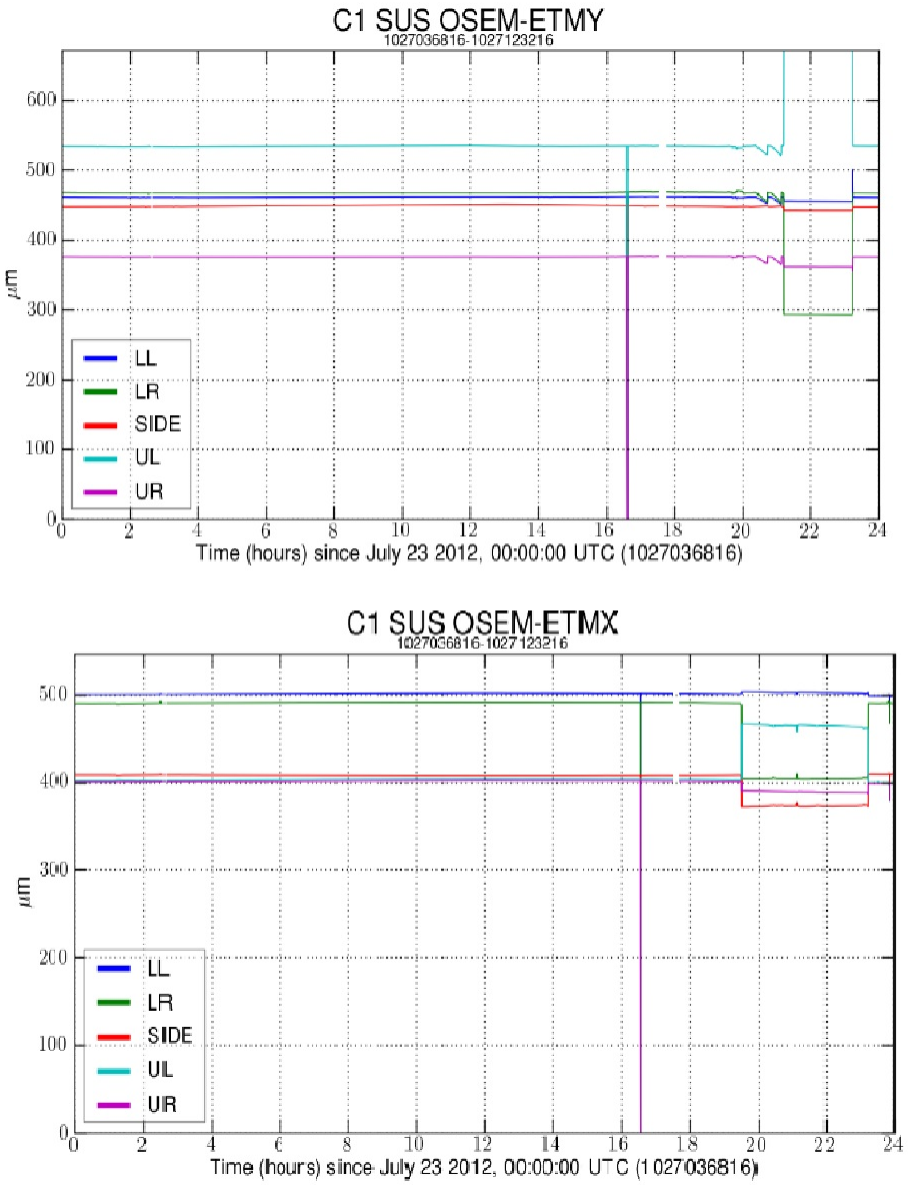

Figure 11: OSEM sensors for the end test masses. There is a disturbance that was common to all of the suspension channels at approximately 4:15 PM PST.

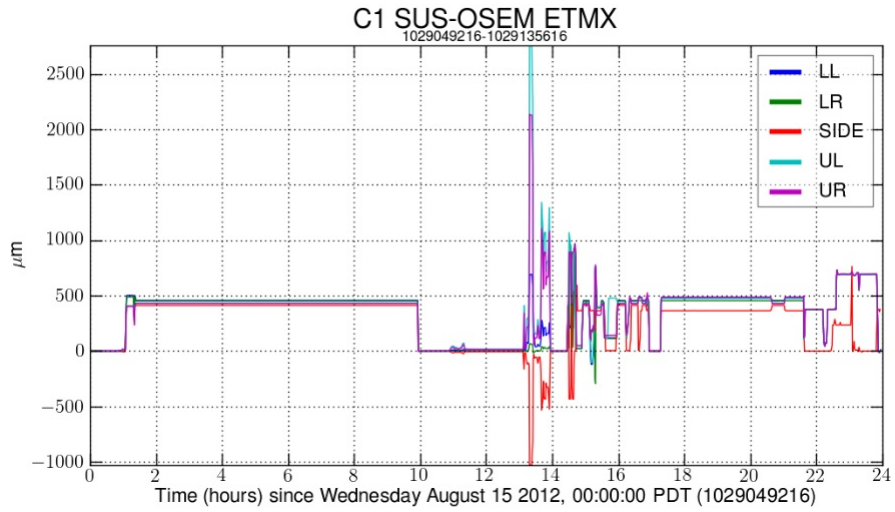

Figure 12: OSEM sensors for the end test.

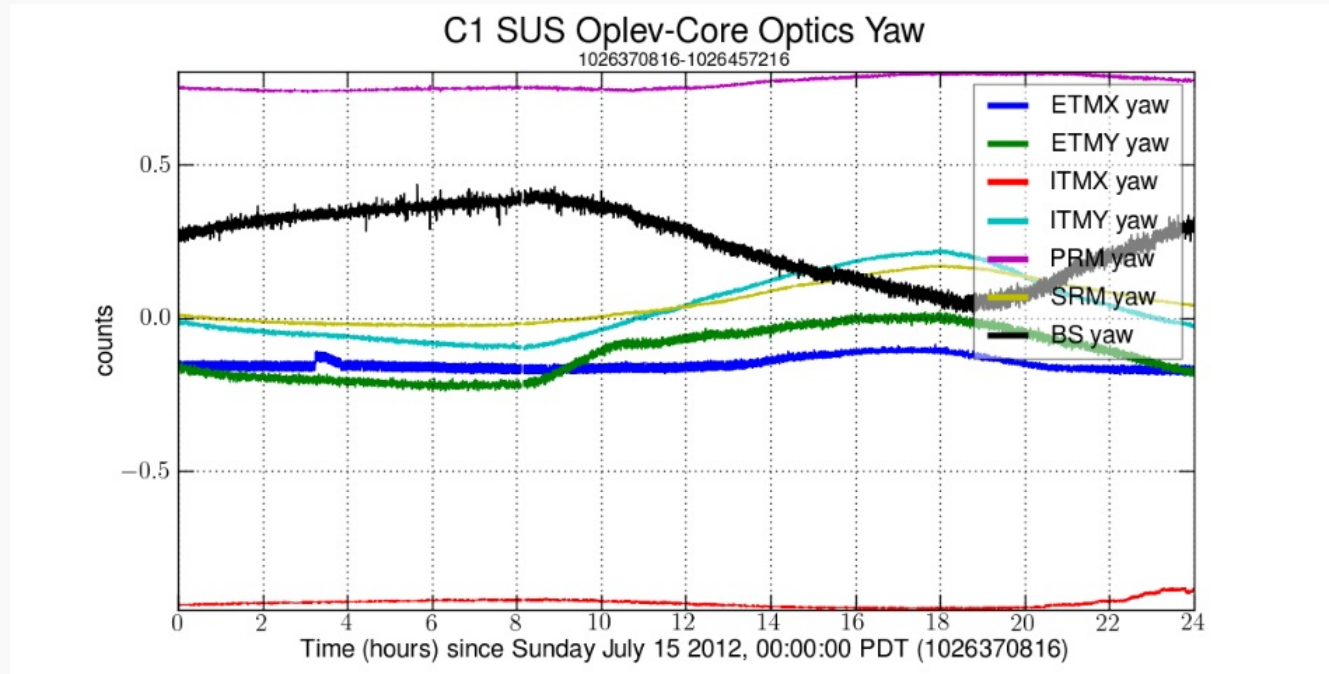

Figure 13: The time-series data for the yaw of all the core optics, as determined by the oplev systems.

wind, the optics might vibrate and add unexpected noise to the data. This would need to be filtered or vetoed from the final information. Additionally, spectrogram plots of time versus frequency on several of the channels are desirable because different frequencies contain separate ranges of information. The signals from the seismic detectors fall into this category. Faraway signals such as ocean waves fall into the low 0.1-0.3 Hz range, while closer vibrations such as rush hour traffic might fall in the 1-3 Hz range.

4.5.1 Vacuum

The entire interferometer at the 40 meter lab is kept in a vacuum of 1010^{-4} Torr. This vacuum system has two types of gauges; cold cathode 423 (CC) gauges that measure the pressure below 10^{-4} Torr and Pirani (P) gauges that measure to 760 Torr and above. The P gauge system is utilized when the interferometer is pumped to atmospheric pressure so the scientists can upgrade and add new parts. The plot of data from the four P gauges when the interferometer is in vacuum can be seen in Figure 14. During this time, the CC gauges are ineffective, but they are informative when the vacuum system is operational. The vacuum tab also includes two Motif Editor and Display Manager (MEDM) screens with essential information about the vacuum system. Although there was a pre-existing page of regularly updating screenshots of several MEDM screens, there was no way to implement images into the summary pages website. I modified the script to include an image option instead of just data plots and was thus able to incorporate all of the MEDM requests from the 40 meter lab. As the cold cathode gauges age, they become insulated and begin to show no ionization current, misleading the system to output unreasonably low pressure values, as in Figure 15. The lab is in the process of acquiring new gauges, but the axes are constrained to only show values down to 10^{-12} Torr until the gauges are replaced. The vacuum pages are fully operational and have been finalized with the commissioners who will be primarily using them.

4.5.2 Seismic

The 40 meter lab has three-axis Gurlap seismometers, Streckeisen seismometers, and Wilcoxson accelerometers that are constantly monitoring the seismic conditions. Band limited root mean square (BLRMS) channels of all of the models are available, although only a few are currently online. The Gurlap BLRMS channels are available for viewing in the real-time projection in the control room at the 40 meter. Each seismometer takes data along three axes, so I included plots of the BLRMS channels for each axis. Calibrated spectrograms of the raw data exist for each axis of every online instrument. Figure 16 is a comparison of the BLRMS channels and the seismic spectrogram. The disturbance around 8:00 PM was a magnitude 7.7 earthquake in the sea of Okhotsk, off the coast of Russia.[10]

4.5.3 Acoustic

Raw data from the microphone channels can be useful if it is portrayed in spectrogram plots such as the example in Figure 17. Acoustic noise interferes with the interferometer by inducing vibrations and potentially shaking the optics out of lock. The thick walls and

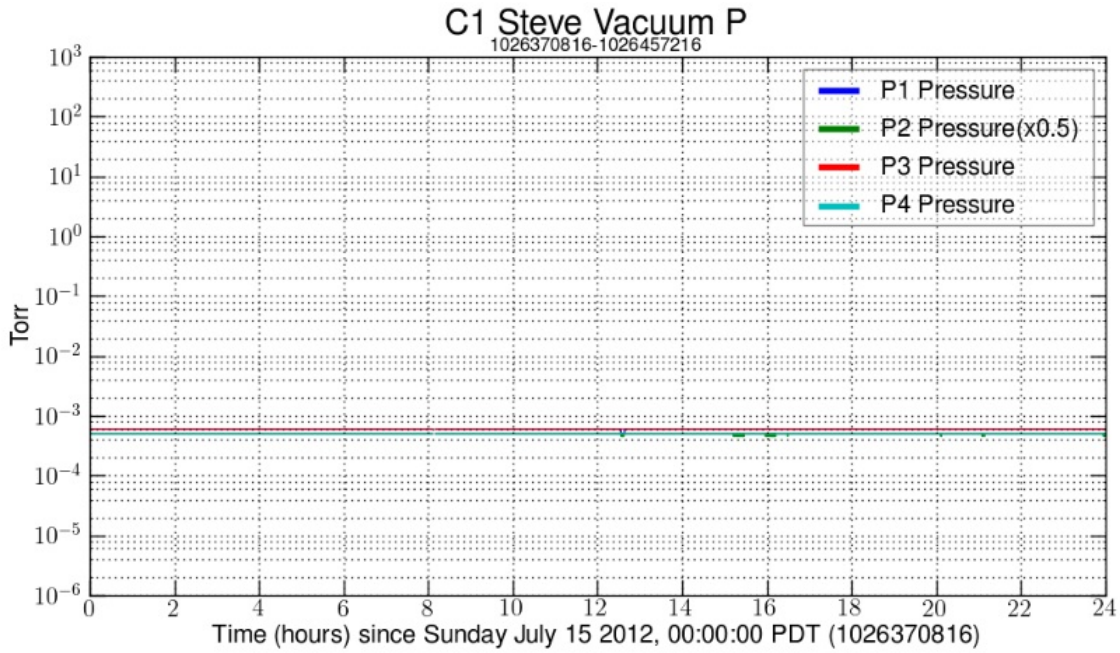

Figure 14: The interferometer vacuum, as measured by the Pirani gauges 1-4. The vacuum is currently operational, so these gauges are all showing the lowest possible reading.

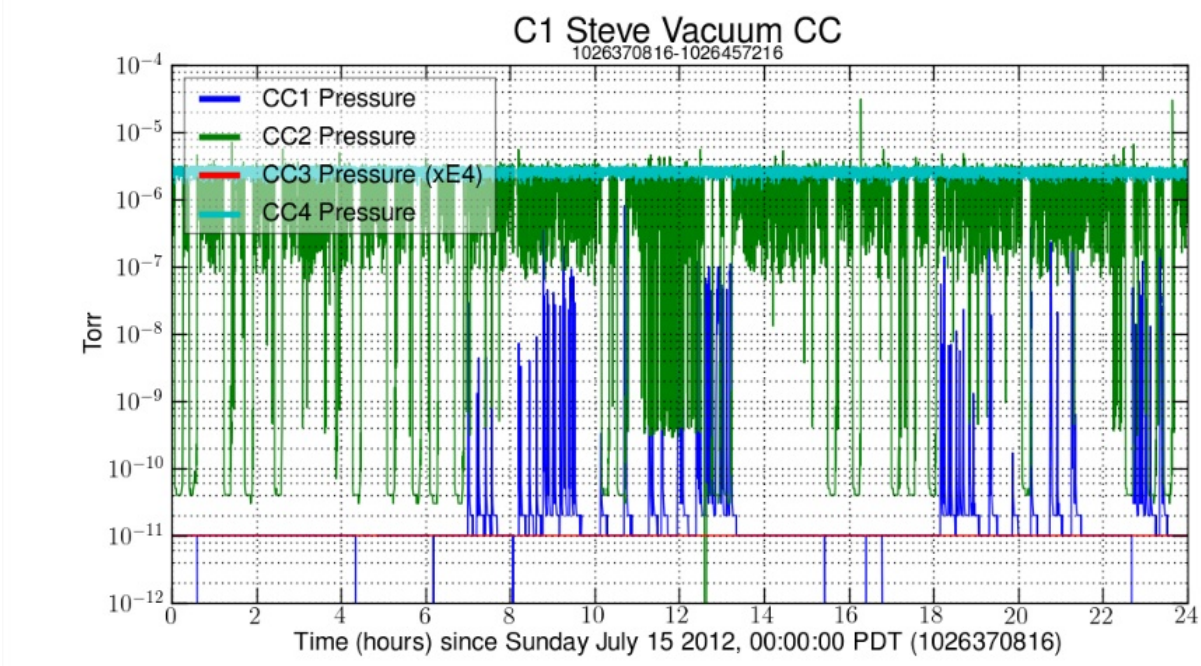

Figure 15: The interferometer vacuum, as measured by the Cold Cathode gauges. These gauges are all in need of replacement, which will significantly improve the continuity of the traces.

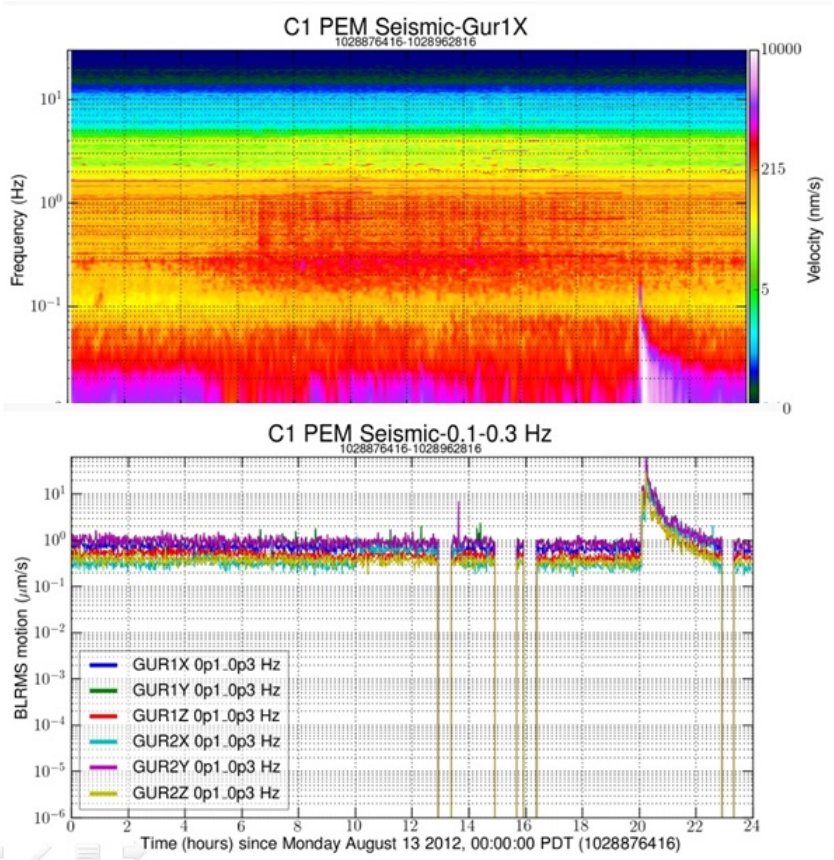

Figure 16: The seismic BLRMS channels for all Gurlap seismometers from 0.1-0.3 Hz and the spectrogram of the GUR1X channel.

vacuum are efficient at limiting acoustic noise but the effects on the components of the interferometer that are less isolated are suspect to interference from acoustic sources. All calibrations for the page were performed using a transfer factor of 39.8107 mV/Pa, as found in the EM 172 manual [11]. A different view of the acoustic channels is obtained by band-limiting the time-series data. In order to display BLRMS traces for the microphone channels, BLRMS channels had to first be created in the controls system. The band-pass filters limit the signal to the frequency range of interest, take the square, pass it through a low-pass filter to exclude frequency-dependent terms, and take the square root. Six channels for each microphone exist, with logarithmic spacing from 1 to 1000 Hz. As of now, only one or two of these channels are outputting relevant data. Audio frequencies range from 20 Hz to 20 kHz, so the channels from 1-3 and 3-10 Hz are very likely to be nothing but noise. Additionally, the sampling frequency for the PEM channels is 2 kHz, which sets the Nyquist frequency at 1 kHz. Thus, the channel from 300- 1000 Hz is expected to experience strange behavior at the Nyquist frequency. To get more relevant data from the microphones, the sampling frequency will be increased from 2 kHz to 16 kHz.

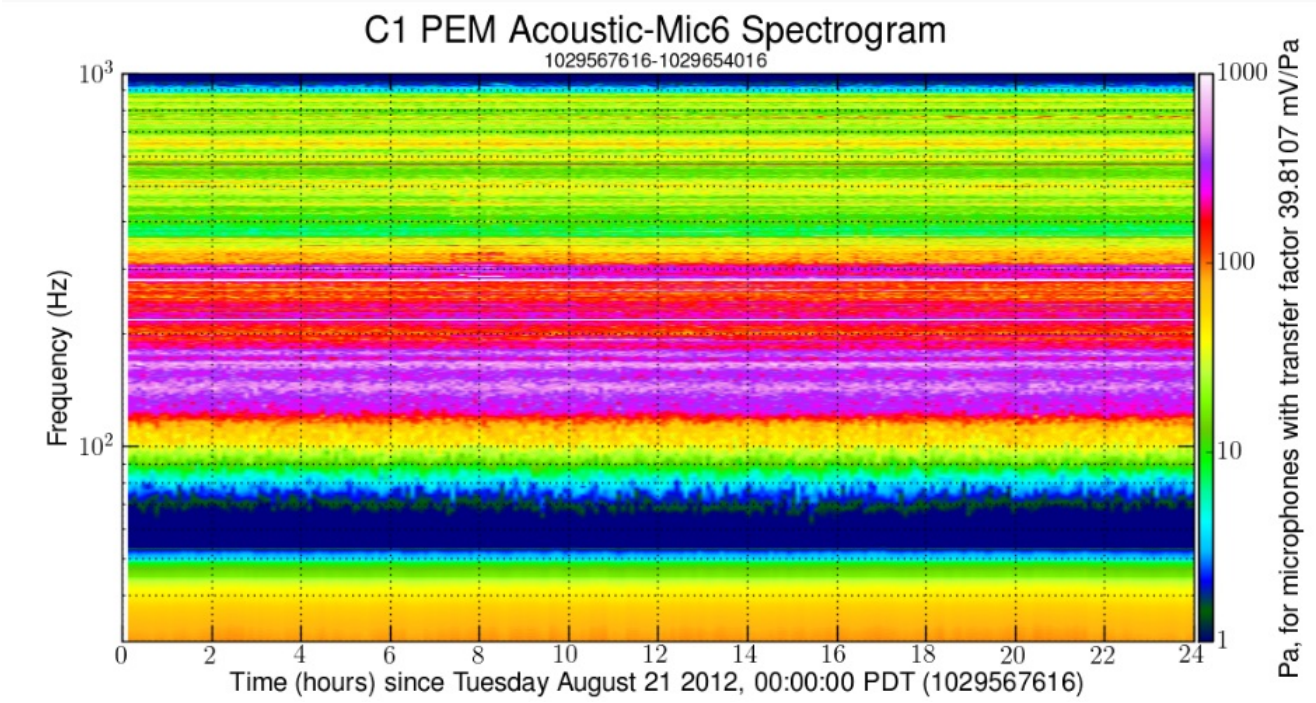

Figure 17: The spectrogram of the PSL Microphone channel.

4.5.4 Weather Station

The Weather Station at the 40 meter lab consists of several monitoring systems located on the roof of the lab and an update screen in the interferometer room. Ideally, the channels from the Weather Station would monitor the interior and exterior temperature, humidity, pressure, wind speed, wind direction and rainfall. Past data trends show the Weather Station was inoperative from mid-2010 onward. The values on the monitor screen in the interferometer

room were accurate, but the computer system was not obtaining any of the data. Fortunately, an article detailed the history of the Weather Station and the location of its components.[12] After the Weather Station components were cleaned, reset and elsewise restored to their initial conditions, the Weather Station channels began showing data again. Figure 18 shows the weather overview, one of the plots on the main Daily Summary page. It includes all data from the Weather Station, multiplied by scalar offsets to produce a cohesive plot.

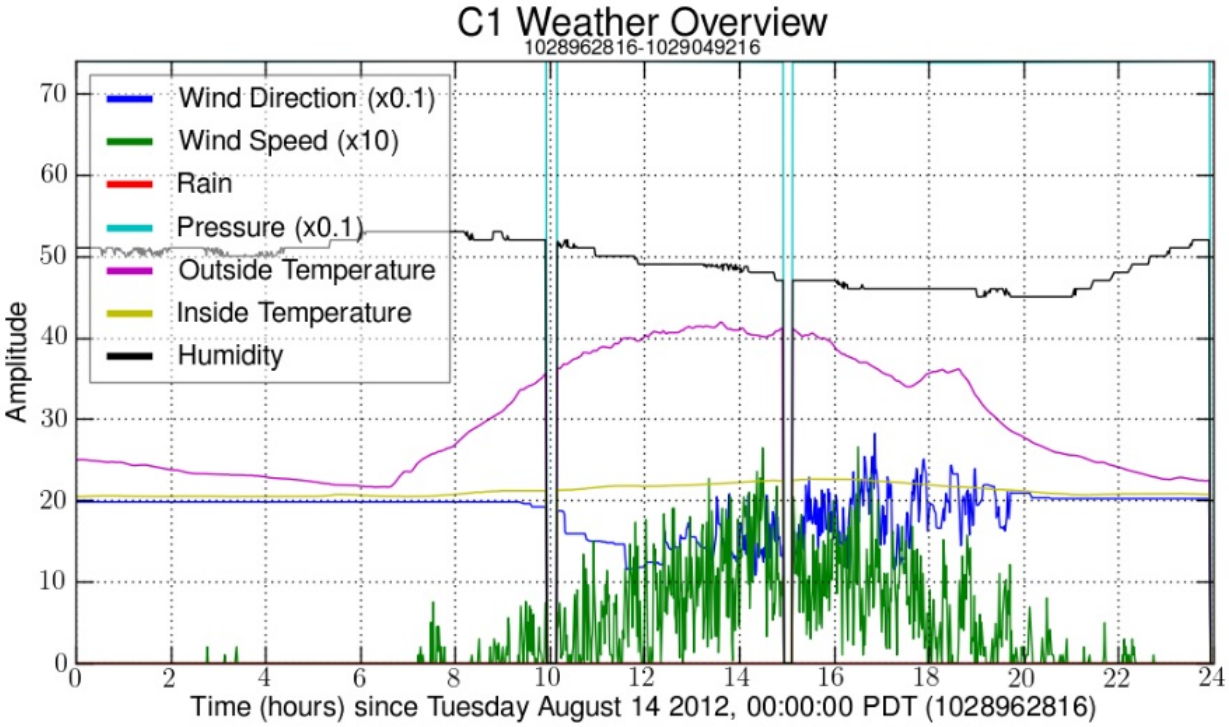

Figure 18: Overview of the information from the Weather Station.

5 Detector Characterization

5.1 Coherence

The coherence between channels over time is an interesting measurement for the scientists at the 40 meter. Some channels, such as the mode cleaner length and PSL microphone, have shown high levels of coherence. The coherence of two channels, x and y, is defined as

$$C_{xy} = \frac{|P_{xy}|^2}{P_{xx}P_{yy}}$$

where P_{xy} is the cross-spectral density of x and y and P_{xx} is the autospectral density of x. Essentially, coherence is a measure of the fractional amount of output power that is produced by an input at a given frequency. In the case of a linear system, the coherence will be equal to one for all frequencies. The coherence plots for the summary pages are spectrogram-style,

with coherence plotted on the z-axis. In order to implement the coherence plot, the data channels must have the same sampling rate.

5.2 Gaussian

Noise at the 40 meter generally assumes a Gaussian distribution but it is essential to characterize the shape of the noise of the important channels. One way to determine whether a noise distribution is Gaussian is the Rayleigh statistic, the normalized variability of the spectral density. This uses the standard deviation and mean of the Power Spectrum

$$S(f) = \frac{1}{N}\sum_{i=1}^{N} |X_i(f)|^2$$

to calculate the Rayleigh statistic for each frequency.

$$R(f) = \frac{\sigma[|X_i(f)|^2]}{\mu[|X_i(f)|^2]}$$

In the instance of perfectly Gaussian noise

$$R(f) = 1 \forall f$$

if the data varies coherently

$$R(f) < 1$$

and if the data is glitchy

$$R(f) > 1$$

Thus, the Rayleigh statistic can be used to characterize Gaussian, glitchy, and stable noise sources. The Rayleighgram plot in the summary pages windows the raw data and takes the fft to find the power spectrum, calculates the mean and standard deviation, computes R and interpolates to fit the log axes. Figure 19 shows the Rayleighgram of data from an OSEM channel.

6 Acknowledgements

I would like to thank my mentors, Jameson Rollins and Rana Adhikari, for their patience and support. In addition, I am grateful to all of the other 40 meter lab members for their advice and information. Specifically, a big thank you to Steve Vass for the Weather Station help, Jenne Driggers for help with the BLRMS mic channels, and Koji Arai for the summary pages template. Finally, I would like to thank Duncan Macleod, the author of the original summary pages script, for writing the original scripts that make it possible to run the pages.

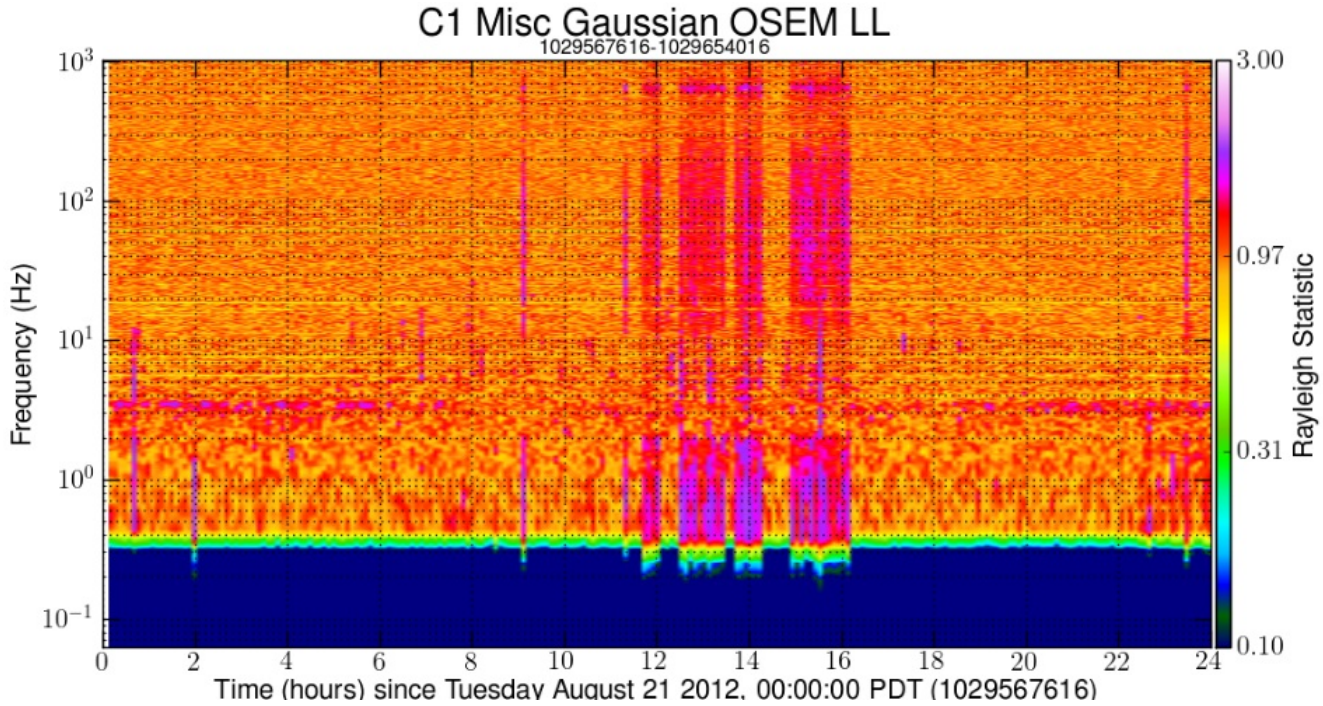

Figure 19: Rayleighgram of the OSEM LL channel. The noise is generally Gaussian, although there are some times that have glitches and certain stable frequency bands.

References

[1] *The Nobel Prize in Physics 1993 Press Release* Web. http://www.nobelprize.org/nobel_prizes/physics/laureates/1993/press.html/#

[2] Saulson, Peter, *Fundamentals of Interferometric Gravitational Wave Detectors*. World Scientific (1994).

[3] *Gravitational Wave* Web. http://gravity.wikia.com/wiki/Gravitational_wave

[4] Ward, Robert *Length Sensing and Control of a Prototype Advanced Interferometric Gravitational Wave Detector* California Institute of Technology (2010).

[5] Driggers, Jenne et. al. *40 Meter Layout* Web. https://dcc.ligo.org/cgi-bin/private/DocDB/ShowDocument?docid=76382

[6] Black, Eric. *Notes on the Pound-Drever-Hall Technique* Web. http://www.ligo.caltech.edu/docs/T/T980045-00.pdf

[7] *New PSL Layout* Web. April 1, 2010 https://dcc.ligo.org/DocDB/0013/G1000699/001/TAC_2010_Jul.pdf

[8] Bonfield, David et. al. *Characterizing the length sensing and control system of the mode cleaner in the LIGO 40m lab* Web. http://www.ligo.caltech.edu/~cit40m/Docs/SURF02/T020147-00.pdf

[9] *LIGO Vocabulary* Web. http://www.ligo.caltech.edu/~ll_news/0607a_news/LIGO_Vocabulary.htm

[10] *Magnitude 7.7 Sea of Okhotsk* USGS. Web. http://earthquake.usgs.gov/earthquakes/recenteqsww/Quakes/usc000bz29.php

[11] *Products and Services: Omni-Directional Electret Microphones* Web. www.primomic.com

[12] *Weather Station* Web. 03 January 2012. http://wiki-40m.ligo.caltech.edu/Weather_Station

[13] Parameswaran, Ajith *On aspects of gravitational-wave detection: Detector characterisation, data analysis and source modelling for ground-based detectors* Leibniz University of Hannover (2007).

[14] Sievers, Lisa, *Seismic Isolation*. Lecture. 6 May 1994 . http://authors.library.caltech.edu/27440/11/12-SEISMIC_ISOLATION.pdf.

[15] Thorne, K. S., Rakhmanov, M et. al., *The Physics of LIGO*. Web. 1994. http://authors.library.caltech.edu/27440/

[16] *Advanced LIGO-Extending the Physics Reach of LIGO*. Web. 9 February 2012. https://www.advancedligo.mit.edu/index.html.

[17] Macleod, Duncan *G1 Summary Page* Web. May 2012. https://atlas1.atlas.aei.uni-hannover.de/~geodc/LSC/monitors/archive_daily/

[18] *40 Meter Wiki Page* Web. May 2012. http://wiki-40m.ligo.caltech.edu

[19] *40 meter Abbreviations and Acronyms* Web. https://dcc.ligo.org/public/0002/M080375/010/LIGO-M080375-V10%20%28Abbreviations%20And%20Acronyms%29.pdf

[20] *Microphone Sensitivity and Conversion* Web. http://www.sengpielaudio.com/calculator-transferfactor.htm

A Intructions for Running and Editing the Summary Pages

The code to run the summary pages is currently located in /users/public_html/40m-summary on the martian network. In this folder, the primary files are a README.txt file that describes some of the details of creating new plots, and the /bin and /share folders that contain essential code for running the program. I will provide a more superficial explanation of the summary pages for the user who only wishes to work with the configuration file, as well as a more in-depth description of changes to the code itself.

The configuration file can be used to make changes in the summary pages content. The file can be found in /users/public_html/40m-summary/share directory/c1_summary_page.ini. To make changes to the glossary, simply add the word you want in the glossary section (line 77), = and the definition. This is straightforward as there are many preexisting entries that can be imitated.

The data plot configuration begins on line 110, where plots can be added and edited. You must provide a channel name (or multiple), labels for each channel, the frame-type (R, T, or M) for full, second or minute trends respectively, and the type of plot desired. The title of each section is of the form [data-TAB-Plot name], where TAB is the name of the tab where the plot will go. All options are set up of the form "option = value". Other available options are amplitude labels and scale factors.

Below the plot configuration are the image setup blocks. Each header must be of the form [image-TAB-name], where TAB is the name of the summary page tab where the plot will go. For the images, tabs must be manually appended in the summary page script (examples can be found in the script if you search "tabs.append((‘Vacuum’, ‘Steve’))". This is because the images do not appear on the summary tabs and only exist under their own headers.

The final section in the configuration file is the plot secion. The plots are organized into dataplots, spectrogramplots, coherenceplots and rayleighplots. More types of plots can be added but modification of the summary pages script is then quite necessary. Within the types of plots, each plot will produce a different representation of data. If you would like two or more different representations (for example, time series and histogram plots) on the same page of the site, simply add the plot names to the data section. The structure of the names is [plotname xcolumn ycolumn zcolumn], where each column represents an axis of the plot.

An example of a plot with two different representations of data:

```
[data-IOO-Yaw]
channels=C1:IOO-MC_TRANS_Y.mean, C1:IOO-WFS1_YAW_OUT16.mean, C1:IOO-WFS2_YAW_OUT16.mean
labels=MC trans. yaw (x100),WFS1 yaw, WFS2 yaw
scale=100, 1, 1
frame-type = M
plot-dataplot1 =
plot-spectrogramplot7 =
```

There is a shell script that can be used to run the summary pages and get frames for any day. This script is /users/public_html/40m-summary/bin/c1_summary_page.sh. To run the pages on current data, use the command:

```
bash /users/public\_html/40m-summary/bin/c1_summary_page.sh now
```

For a past day, say May 30 2012:

```
bash /users/public_html/40m-summary/bin/c1_summary_page.sh 2012/05/30
```

One thing to be cautious of while running the script is that, if a day from a previous month is the most recent date run, all subsequent months will disappear from the calendar on the website. They will reappear when a current page is run. The pages contain all the available data since their creation, so running pages in the past shouldn't to be a regular issue. The bash script generates caches of all the data for that day (with appropriate edits for Daylight Saving's Time) and runs the summary page script with that data.

The python file /users/public_html/40m-summary/bin/summary_page.py contains the main summary pages script. There are several sections of this file that are never used at the 40 meter lab, as there are no segments or triggers. All of the times have been changed from UTC time to PST/PDT time, to make it more intuitive for lab members. There is a git repository that tracks all of the changes in the script, and additional changes can be found in the git repository in the dailySummary file in the elizabeth davison user folder.

There are a few specific functions in the script that are useful to understand for more serious editing. The summary_page function at the end of the file calls all of the others and sets up tabs and organization of the website. To add tabs to the site, or if a new section needs to be added, simply add the tab name to the parent list. Then, if the new tab is used in the configuration file, it will appear on the site.

```
# here we define applicable parents
parents = ['Summary', 'PSL','IOO','IFO','Acoustic','PEM',
          'Seismic','SUS-OPLEV','SUS-OSEM','PEM', 'Steve',\
          'Weather','Misc']
```

The other useful functions are get_data, process_data, and the functions that they call based on the type of plots requested by the user. Two auxiliary files, new_dqPlotUtils.py and new_dqDataUtils.py, are used to organize and plot the data from the frames in the cache. These are the necessary files for running and editing the summary pages and can all be accessed and run on the martian network.

A final suggestion towards getting the coherence plots to work is updating the pylal.seriesutils library to include the "resample" function for the REAL8TimeSeries data. Once this is accomplished, the code should work. If there are issues, the best places to check would be in the get_coherence function.

B Rayleighgram Code

```
def Rayleigh(data, fs, NFFT=256, overlap=128,\
                              window=('kaiser',24), sides='onesided',\
                              verbose=False, log=False, warn=True):

  """
    Computes Rayleigh statistic of a data series.
  """

  if sides!='onesided':
    raise NotImplementedError('Only one sided spectrum implemented for the moment')

  # cast data series to numpy array
  data = numpy.asarray(data)

  # number of segments (must be even)
  if overlap==0:
    numseg = int(len(data)/NFFT)
  else:
    numseg = 1 + int((len(data)-NFFT)/overlap)
  assert (numseg - 1)*overlap + NFFT == len(data),\
         "Data is wrong length to be covered completely, please resize"


  # construct window
  win = scipy.signal.get_window(window, NFFT)

  if verbose: sys.stdout.write("%s window constructed.\nConstructing "
                               "median-mean average spectrum "
                               "with %d segments...\n"\
                               % (window, numseg))

  #
  # construct PSD
  #

  # fft scaling factor for units of Hz^-1
  scaling_factor = 1 / (fs * NFFT)

  # construct frequency
  f = numpy.arange(NFFT//2 + 1) * (fs / NFFT)

  # if odd number of segments, ignore the first one (better suggestions welcome)
  if numseg == 1:
    odd = [0]
```

```
  even = []
elif numseg % 2 == 1:
  odd = odd[:-1]
  numseg -= 1
  if warn:
    sys.stderr.write("WARNING: odd number of FFT segments, skipping last.\n")

# get bias factor
biasfac = MedianBias(numseg//2)
# construct normalisation factor
normfac = 1/(2*biasfac)

# set data holder
S = numpy.empty((numseg, len(f)))

# loop over segments
for i in xrange(numseg):

  # get data
  chunk = data[i*overlap:i*overlap+NFFT]
  # apply window
  wdata = WindowDataSeries(chunk, win)
  # FFT
  S[i]  = PowerSpectrum(wdata, sides) * scaling_factor

if verbose: sys.stdout.write("Generated spectrum for each chunk.\n")

# compute median-mean average
if numseg > 1:
  mu = numpy.mean([S[i] for i in range(numseg-1)],0)
  sigma = numpy.std([S[i] for i in range(numseg-1)],0)
  R = sigma/mu
else:
  R = S.flatten()
if verbose: sys.stdout.write("Calculated mean.\n")

if log:
  f_log = numpy.logspace(numpy.log10(f[1]), numpy.log10(f[-1]), num=len(f)/2,\
                         endpoint=False)
  I = interpolate.interp1d(f, R)
  R = I(f_log)
  return f_log, R

return f, R
```